

# **CHAPTER 3**

## **MODELING OF A CONSTANT $D_0$ CONTROLLED BOOSTBUCK RECTIFIER**

### **3.1 Introduction**

From rough review of the time varying  $d_0$  controlled rectifier in the previous chapter, one can see that, first, it is desired to propose a bidirectional power flow topology. Next, from the viewpoint of simplified implementation and robust control, a constant  $D_0$  control strategy is indeed necessary. Hence, in this chapter an improved topology which replaces the power diode of [12, 42] with another active switch is proposed to achieve bidirectional power flow capability. Then, motivated by the approximated equivalent DC duty ratio for the generalized zero voltage space vectors presented in [12, 42], the author derives the closed form duty ratio functions for the seven active switches by using the familiar state averaging technique. Then the DC model and small signal models are derived by perturbation and linearization after a coordinate transformation. However, the corresponding equivalent circuit model will be given in the next chapter. Finally, some simulation results are presented for demonstrating the validity of the proposed constant  $D_0$  control strategy for the new converter.

### **3.2. Derivation of the Closed Form Duty Cycle Control Laws**

Fig. 3.1 shows the proposed three-phase step up/down AC/DC converter where  $S_1, S_2, \dots, S_7$  are the active switches and  $R_s$  is the ESR of  $L_s$ . Unlike the six switches in three-phase boost AC/DC converters where the upper and the lower switches of each bridge arm are not allowed to be shorted, the first six active switches in Fig. 3.1 can be operated independently.

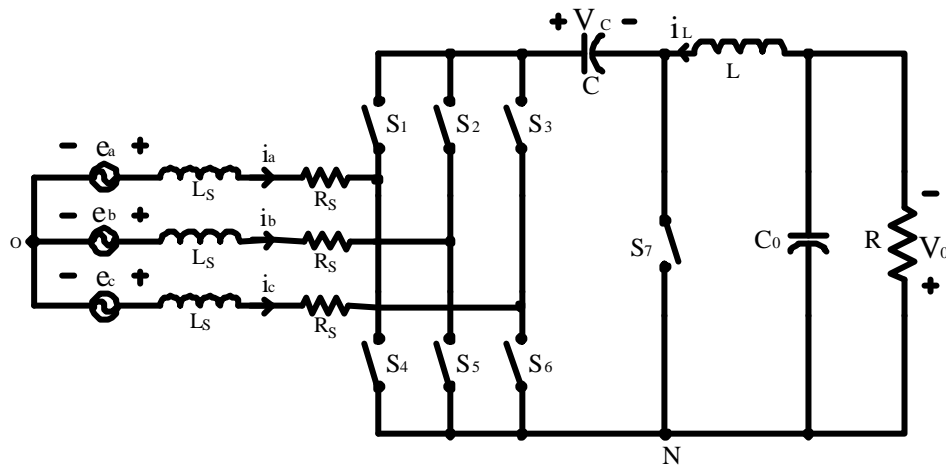


Fig. 3.1 Power circuit of the proposed step up/down AC/DC converter

Based on the motivation of equivalent DC duty cycle in [12, 42], Fig. 3.2 shows conceptual gating signals of seven switches for one switching period  $T_s$ . From Fig. 3.2 one can see that during each switching period there is one portion, namely  $d_0 T_s$ , where all six active switches of the bridge are closed such that  $v_c$  of Fig. 3.1 can be discharged to supply the output to keep the DC stage worked as a C'uk converter. The reason of turning on six switches, corresponding to applying  $V_{77}$  space voltage vector in [12, 42], is to minimize the conduction loss. Also, to keep the function of

C'uk converter,  $S_7$  should operate complementary for the remaining switching period, namely  $(1-d_0)T_s$ , where all six switches of the bridge function basically as that of a boost type converter [10] to charge  $C$ . Assume that the switching frequency is much higher than the AC line frequency. Then, one can use the state space averaging technique [43] to get the following averaged equation.

$$\begin{bmatrix} \frac{di_a}{dt} \\ \frac{di_b}{dt} \\ \frac{di_c}{dt} \\ \frac{di_L}{dt} \\ \frac{dv_C}{dt} \\ \frac{dv_o}{dt} \end{bmatrix} = \begin{bmatrix} \frac{-R_s}{L_s} & 0 & 0 & 0 & \frac{-d_1}{L_s} & 0 \\ 0 & \frac{-R_s}{L_s} & 0 & 0 & \frac{-d_2}{L_s} & 0 \\ 0 & 0 & \frac{-R_s}{L_s} & 0 & \frac{-d_3}{L_s} & 0 \\ 0 & 0 & 0 & 0 & \frac{1-d_7}{L} & \frac{-1}{L} \\ \frac{d_1}{C} & \frac{d_2}{C} & \frac{d_3}{C} & \frac{-(1-d_7)}{C} & 0 & 0 \\ 0 & 0 & 0 & \frac{1}{C_0} & 0 & \frac{-1}{RC_0} \end{bmatrix} \begin{bmatrix} i_a \\ i_b \\ i_c \\ i_L \\ v_C \\ v_o \end{bmatrix} + \frac{1}{L_s} \begin{bmatrix} e_a \\ e_b \\ e_c \\ 0 \\ 0 \\ 0 \end{bmatrix} - \frac{1}{L_s} \begin{bmatrix} 1 \\ 1 \\ 1 \\ 0 \\ 0 \\ 0 \end{bmatrix} v_{NO} \quad (3.1)$$

For simplicity, the equivalent series resistance (ESR) of  $C$ ,  $C_o$  and  $L$  are neglected in the above derivation. From Kirchhoff's current law,  $i_a + i_b + i_c = 0$ , and the upper half of equation (3.1) it is straightforward to get

$$v_{NO} = -\frac{1}{3}(d_1 + d_2 + d_3)v_C \quad (3.2)$$

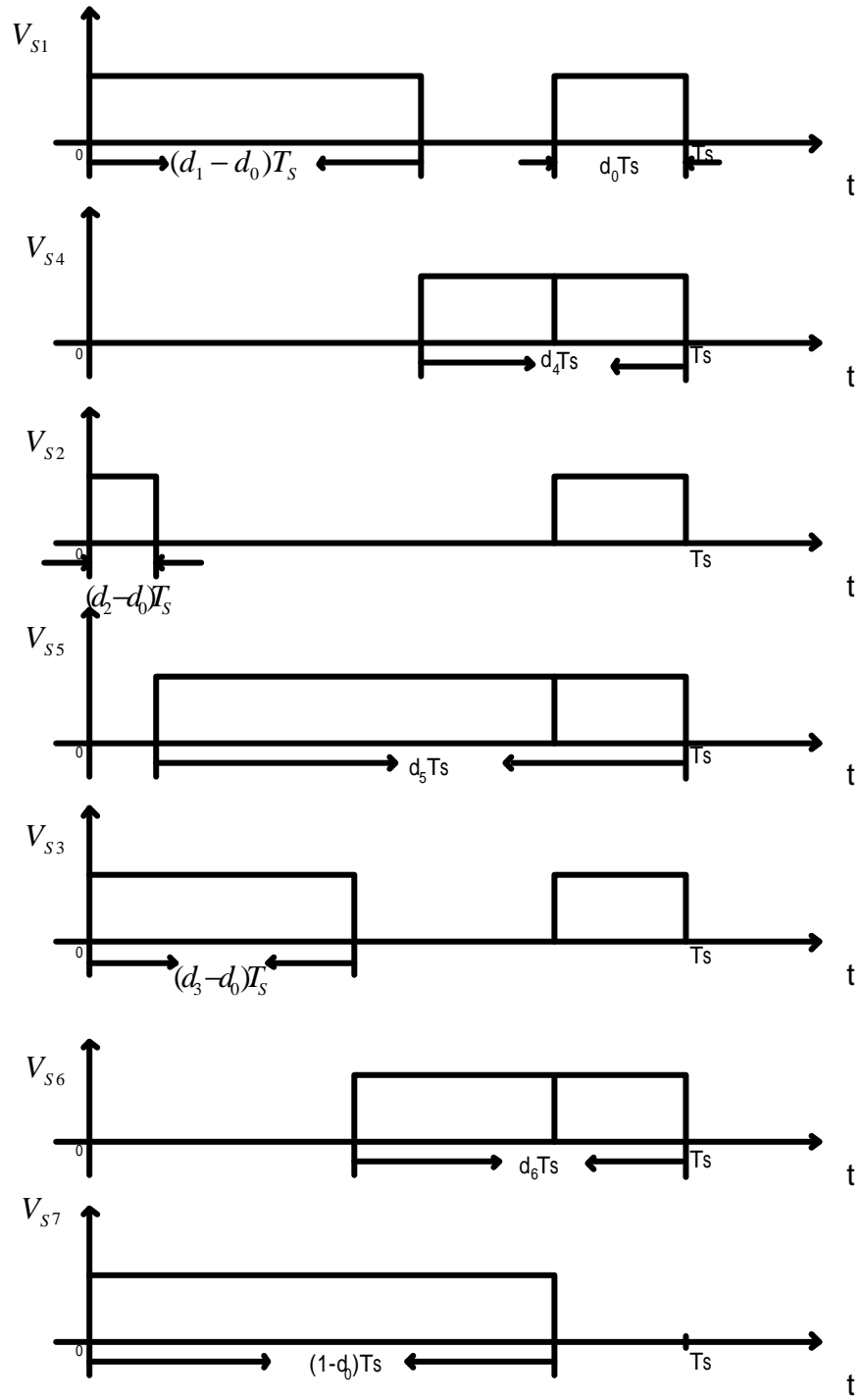


Fig. 3.2 Conceptual gating signals of seven switches

As can be observed from Figs. 3.1 and 3.2, in order to preserve the dc C'uk converter operation principle, the full bridge is allowed to be short circuited with an equivalent DC duty cycle  $1-d_7$ . Thus, for convenience, one can define the duty cycles as follows:

$$\begin{aligned} d_0 &= 1-d_7, \\ d_k &= \frac{1+d_0+m_k(t)}{2}, \\ d_{k+3} &= \frac{1+d_0-m_k(t)}{2}, \quad k=1, 2, 3 \end{aligned} \quad (3.3)$$

where  $m_k(t)$ ,  $k=1,2,3$  are the time varying part modulation indices to be decided, and

$$\begin{aligned} 0 &\leq |m_k(t)| \leq 1 \\ d_0 + d_k + d_{k+3} &= 1+d_0, \quad k=1, 2, 3 \end{aligned} \quad (3.4)$$

Then, by substituting equations (3.2) and (3.3) into (3.1), one has the following form.

$$\frac{dX}{dt} = \begin{bmatrix} A_1 & A_2 \\ A_3 & A_4 \end{bmatrix} X + BU \quad (3.5)$$

where

$$X = [i_a \ i_b \ i_c \ i_L \ v_C \ v_o]^T, \quad A_1 = \text{diag} \left[ \frac{-R_s}{L_s} \ \frac{-R_s}{L_s} \ \frac{-R_s}{L_s} \right]$$

$$A_2 = \begin{bmatrix} 0 & \frac{-m_1}{2L_{s1}} & 0 \\ 0 & \frac{-m_2}{2L_s} & 0 \\ 0 & \frac{-m_3}{2L_s} & 0 \end{bmatrix}, \quad A_3 = \begin{bmatrix} 0 & 0 & 0 \\ \frac{m_1}{2C} & \frac{m_2}{2C} & \frac{m_3}{2C} \\ 0 & 0 & 0 \end{bmatrix}$$

$$A_4 = \begin{bmatrix} 0 & \frac{d_0}{L} & \frac{-1}{L} \\ \frac{-d_0}{C} & 0 & 0 \\ \frac{1}{C_0} & 0 & \frac{-1}{RC_0} \end{bmatrix}, \quad B = \begin{bmatrix} \frac{1}{L_s} & 0 & 0 \\ 0 & \frac{1}{L_s} & 0 \\ 0 & 0 & \frac{1}{L_s} \\ 0 & 0 & 0 \\ 0 & 0 & 0 \\ 0 & 0 & 0 \end{bmatrix}$$

$$U = [e_a \ e_b \ e_c]^T$$

Next, assume that

$$\begin{aligned} e_a &= E_m \cos \mathbf{w}t & , & \quad i_a = I_m \cos(\mathbf{w}t - \mathbf{f}) \\ e_b &= E_m \cos(\mathbf{w}t - 120^0) & , & \quad i_b = I_m \cos(\mathbf{w}t - \mathbf{f} - 120^0) \\ e_c &= E_m \cos(\mathbf{w}t + 120^0) & , & \quad i_c = I_m \cos(\mathbf{w}t - \mathbf{f} + 120^0) \end{aligned} \quad (3.6)$$

where a phase shift  $\mathbf{f}$  is included in line currents for generality.

It follows from equations (3.5)-(3.6) and under steady state that one can obtain the following solution:

$$\begin{aligned} \frac{m_k(t)}{2} = & \frac{1}{v_c} [E_m \cos(\mathbf{w}t - (k-1)120^\circ) - R_s I_m \cos(\mathbf{w}t - \mathbf{f} - (k-1)120^\circ) \\ & + \mathbf{w}L_s I_m \sin(\mathbf{w}t - \mathbf{f} - (k-1)120^\circ)] \quad , \quad k = 1, 2, 3 \end{aligned} \quad (3.7)$$

Therefore the desired closed form duty functions of equation (3.3) can be obtained easily. Also, one can see that by using the above algebraic approach the coordination of seven switches can be achieved automatically. Finally, it may be worth mentioning that for a desired output voltage the choice of  $d_0$ , and hence  $d_7$  also, is not unique as can be seen in later sections.

### 3.3. Low Frequency DC and AC Models

For simplicity, define the following space vectors first:

$$\mathbf{e}_s^\times = \sqrt{\frac{2}{3}}(e_a + a e_b + a^2 e_c) = \sqrt{\frac{3}{2}} E_m e^{j\mathbf{w}t} \quad (3.8)$$

$$\mathbf{i}_s^\times = \sqrt{\frac{2}{3}}(i_a + a i_b + a^2 i_c) = \sqrt{\frac{3}{2}} I_m e^{j(\mathbf{w}t - \mathbf{f})} \quad (3.9)$$

$$\mathbf{d}_s^\times = \sqrt{\frac{2}{3}}(d_1 + a d_2 + a^2 d_3) = \sqrt{\frac{3}{2}} d_m e^{j(\mathbf{w}t - \mathbf{j})} \quad (3.10)$$

where

$$a \equiv e^{j\frac{2\pi}{3}}$$

$$[e_a \ e_b \ e_c] = \sqrt{\frac{2}{3}} \text{Re}\{[1 \ a^2 \ a] \check{e}_s^\times\}$$

$$[i_a \ i_b \ i_c] = \sqrt{\frac{2}{3}} \text{Re}\{[1 \ a^2 \ a] \check{i}_s^\times\}$$

$$[\frac{m_1}{2} \ \frac{m_2}{2} \ \frac{m_3}{2}] = \sqrt{\frac{2}{3}} \text{Re}\{[1 \ a^2 \ a] \check{d}_s^\times\}$$

Thus, application of the above notation to equation (3.5) yields

$$\frac{d\check{i}_s^\times}{dt} = -\frac{R_s}{L_s} \check{i}_s^\times - \frac{v_c}{L_s} \check{d}_s^\times + \frac{1}{L_s} \check{e}_s^\times \quad (3.11)$$

$$\frac{di_L}{dt} = \frac{d_0}{L} v_c - \frac{1}{L} v_0 \quad (3.12)$$

$$\frac{dv_c}{dt} = \frac{1}{C} \text{Re}[\check{i}_s^\times \check{d}_s^{\times*}] - \frac{d_0}{C} i_L \quad (3.13)$$

$$\frac{dv_0}{dt} = \frac{1}{C_0} i_L - \frac{1}{RC_0} v_0 \quad (3.14)$$

where  $*$  denotes the complex conjugation and  $i_a + i_b + i_c = 0$  has been applied to obtain the above equation. Next, transforming  $\check{i}_s^\times, \check{d}_s^\times$  into the synchronously rotating reference frame, i.e. define

$$\begin{aligned} \check{i}_s^\times &\equiv (I_d + jI_q) e^{j\omega t} \\ \check{d}_s^\times &\equiv (d_d + jd_q) e^{j\omega t} \end{aligned}$$

where  $I_d + jI_q$  and  $d_d + jd_q$  are phasors in the new coordinate.



Then one can obtain the following equation

$$\frac{d}{dt} \begin{bmatrix} I_d \\ I_q \\ i_L \\ v_C \\ v_0 \end{bmatrix} = \begin{bmatrix} \frac{-R_s}{L_s} & \mathbf{w} & 0 & \frac{-d_d}{L_s} & 0 \\ -\mathbf{w} & \frac{-R_s}{L_s} & 0 & \frac{-d_q}{L_s} & 0 \\ 0 & 0 & 0 & \frac{d_0}{L} & \frac{-1}{L} \\ \frac{d_d}{C} & \frac{d_q}{C} & \frac{-d_0}{C} & 0 & 0 \\ 0 & 0 & \frac{1}{C_0} & 0 & \frac{-1}{RC_0} \end{bmatrix} \begin{bmatrix} I_d \\ I_q \\ i_L \\ v_C \\ v_0 \end{bmatrix} + \begin{bmatrix} \frac{1}{L_s} \\ 0 \\ 0 \\ 0 \\ 0 \end{bmatrix} E_m \quad (3.15)$$

where

$$\begin{aligned} I_d &= \sqrt{\frac{3}{2}} I_m \cos \mathbf{f} & I_q &= -\sqrt{\frac{3}{2}} I_m \sin \mathbf{f} \\ d_d &= \sqrt{\frac{3}{2}} d_m \cos \mathbf{j} & d_q &= -\sqrt{\frac{3}{2}} d_m \sin \mathbf{j} \end{aligned}$$

Finally, to obtain the DC and the small signal model, one can apply the following perturbations:

$$\begin{aligned} I_d &= I_{d0} + \hat{I}_d & I_q &= I_{q0} + \hat{I}_q \\ v_C &= V_C + \hat{v}_C & i_L &= I_L + \hat{i}_L \\ v_0 &= V_0 + \hat{v}_0 & E_m &= E_{m0} + \hat{E}_m \\ d_d &= D_d + \hat{d}_d & d_q &= D_q + \hat{d}_q \\ d_0 &= D_0 + \hat{d}_0 \end{aligned}$$

Application of the above equations to equation (3.15) and neglect higher order terms

yield the following DC and small signal models:

$$D_d = \frac{1}{V_c}(E_m - R_s I_d + \mathbf{w} L_s I_q) \quad (3.16)$$

$$D_q = \frac{1}{V_c}(-R_s I_q - \mathbf{w} L_s I_d) \quad (3.17)$$

$$D_0 = \frac{(D_d I_d + D_q I_q)}{I_L} \quad (3.18)$$

$$V_0 = D_0 V_c \quad (3.19)$$

$$I_L = \frac{V_0}{R} \quad (3.20)$$

$$\begin{aligned} \frac{d}{dt} \begin{bmatrix} \hat{I}_d \\ \hat{I}_q \\ \hat{i}_L \\ \hat{v}_c \\ \hat{v}_0 \end{bmatrix} &= \begin{bmatrix} \frac{-R_s}{L_s} & \mathbf{w} & 0 & \frac{-D_d}{L_s} & 0 \\ -\mathbf{w} & \frac{-R_s}{L_s} & 0 & \frac{-D_q}{L_s} & 0 \\ 0 & 0 & 0 & \frac{D_0}{L} & \frac{-1}{L} \\ \frac{D_d}{C} & \frac{D_q}{C} & \frac{-D_0}{C} & 0 & 0 \\ 0 & 0 & \frac{1}{C_0} & 0 & \frac{-1}{RC_0} \end{bmatrix} \begin{bmatrix} \hat{I}_d \\ \hat{I}_q \\ \hat{i}_L \\ \hat{v}_c \\ \hat{v}_0 \end{bmatrix} + \begin{bmatrix} \frac{-V_c}{L_s} & 0 & 0 \\ 0 & \frac{-V_c}{L_s} & 0 \\ 0 & 0 & \frac{V_c}{L} \\ \frac{I_{d0}}{C} & \frac{I_{q0}}{C} & \frac{-I_L}{C} \\ 0 & 0 & 0 \end{bmatrix} \begin{bmatrix} \hat{d}_d \\ \hat{d}_q \\ \hat{d}_0 \end{bmatrix} \\ &+ \begin{bmatrix} \frac{1}{L_s} & 0 & 0 & 0 & 0 \end{bmatrix}^T \hat{E}_m \end{aligned} \quad (3.21)$$

From the above DC model, one can see the meanings of  $D_0$ . Basically, it is not only related to  $V_o$  and  $V_c$  but also dependent on the AC line currents,  $I_L$  and the duty cycles of first six active switches. In fact, from equations (3.16) to (3.20) one can

obtain the following results. And the equivalent circuit will be shown in chapter 4.

$$\frac{3}{2}E_m I_m \cos \mathbf{f} = \frac{V_o^2}{R} + \frac{3}{2}I_m^2 R_s \quad (3.22)$$

$$D_d = \frac{D_0}{V_o}(E_m - R_s I_d + \mathbf{w} L_s I_q) \quad (3.23)$$

$$D_q = \frac{D_0}{V_o}(-R_s I_q - \mathbf{w} L_s I_d) \quad (3.24)$$

Equation (3.22) actually represents the principle of conservation of power. From equations (3.23) and (3.24) one can see that for a given output voltage  $V_o$ ,  $D_d$  and  $D_q$  can be obtained by choosing a proper value of  $D_0$  which satisfies the following inequality

$$1 - D_0 \geq 2D_m \equiv 2\sqrt{\frac{2}{3}}\sqrt{D_d^2 + D_q^2} \quad (3.25)$$

as can be seen from equation (3.3) to guarantee a positive value duty cycle.

Similarly, from the state equation of (3.21) one can take Laplace transform to get the desired transfer functions. For example, the duty cycle control to output transfer functions take the following forms:

$$T_d(s) \equiv \frac{\hat{v}_o(s)}{\hat{d}_d(s)} = \frac{1}{\Delta} \left( \frac{-V_c}{L_s} b_1 + \frac{I_{do}}{C} b_4 \right)$$

$$T_q(s) \equiv \frac{\hat{v}_o(s)}{\hat{d}_q(s)} = \frac{1}{\Delta} \left( \frac{-V_c}{L_s} b_2 + \frac{I_{qo}}{C} b_4 \right)$$

$$T_0(s) \equiv \frac{\hat{v}_o(s)}{\hat{d}_0(s)} = \frac{1}{\Delta} \left( \frac{V_c}{L} b_3 + \frac{-I_L}{C} b_4 \right)$$

$$T_{em}(s) \equiv \frac{\hat{v}_o(s)}{\hat{E}_m(s)} = \frac{1}{\Delta} \left( \frac{1}{L_s} b_1 \right)$$

where

$$\Delta = s^5 + a_4 s^4 + a_3 s^3 + a_2 s^2 + a_1 s + a_0$$

$$a_4 = \frac{1}{RC_0} + \frac{2R_s}{L_s}$$

$$a_3 = \frac{1}{LC_0} + \frac{2R_s}{RL_s C_0} + \frac{R_s^2}{L_s^2} + \mathbf{w}^2 + \frac{(D_d^2 + D_q^2)}{L_s C} + \frac{D_0^2}{LC}$$

$$a_2 = \frac{2R_s}{L_s LC_0} + \frac{R_s^2}{RC_0 L_s^2} + \frac{\mathbf{w}^2}{RC_0} + \frac{(D_d^2 + D_q^2)}{RL_s CC_0} + \frac{R_s(D_d^2 + D_q^2)}{L_s^2 C} + \frac{D_0^2}{RLCC_0} + \frac{2R_s D_0^2}{L_s LC}$$

$$a_1 = \frac{(D_d^2 + D_q^2)}{L_s LCC_0} + \frac{R_s(D_d^2 + D_q^2)}{RL_s^2 CC_0} + \frac{\mathbf{w}^2}{LC_0} + \frac{R_s^2}{L_s^2 LC_0} + \frac{2R_s D_0^2}{RL_s LCC_0} + \frac{R_s^2 D_0^2}{L_s^2 LC} + \frac{\mathbf{w}^2 D_0^2}{LC}$$

$$a_0 = \frac{R_s(D_d^2 + D_q^2)}{L_s^2 LCC_0} + \frac{R_s^2 D_0^2}{RL_s^2 LCC_0} + \frac{\mathbf{w}^2 D_0^2}{RLCC_0}$$

$$b_1 = \frac{D_0 D_d}{LCC_0} s + \frac{D_0}{LCC_0} \left( \frac{D_d R_s}{L_s} - D_q \mathbf{w} \right)$$

$$b_2 = \frac{D_0 D_q}{LCC_0} s + \frac{D_0}{LCC_0} \left( \frac{D_q R_s}{L_s} + D_d \mathbf{w} \right)$$

$$b_3 = \frac{1}{C_0} s^3 + \frac{2R_s}{L_s C_0} s^2 + \left( \frac{R_s^2}{L_s^2 C_0} + \frac{(D_d^2 + D_q^2)}{L_s CC_0} + \frac{\mathbf{w}^2}{C_0} \right) s + \frac{R_s(D_d^2 + D_q^2)}{L_s^2 CC_0}$$

$$b_4 = \frac{D_0}{LC_0} s^2 + \frac{2D_0 R_s}{L_s LC_0} s + \frac{D_0}{LC_0} \left( \frac{R_s^2}{L_s^2} + \mathbf{w}^2 \right)$$

### 3.4. Some Numerical Simulation Results

To facilitate the understanding of the above theoretical results, some simulation results are given below as illustrations. The parameters of the converter in Fig. 3.1 are listed below for reference.

$$L_s = L = 7.5 \text{ mH} , \quad C = C_o = 820 \mu\text{F}$$

$$R_s = 0.45 \Omega , \quad P_o = \frac{V_o^2}{R} = 4 \text{ kW}$$

AC line frequency 60 Hz

$$\text{Phase voltage amplitude } \frac{220\sqrt{2}}{\sqrt{3}} \text{ volts}$$

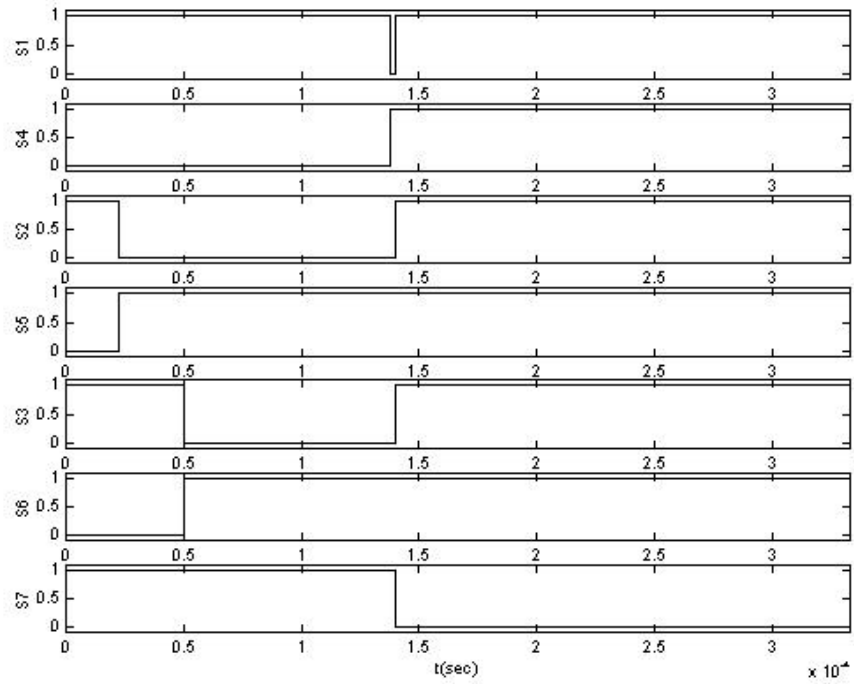
Power factor = 1.0

The seven active switches are considered as ideal in the simulation process. The sawtooth wave frequency is 3 kHz. It may be worth mentioning that the duty ratio of  $d_0$  is generated by comparing with a negative slope sawtooth wave. Thus, the duty ratio of  $S_7$  is obtained by inverting the output again.

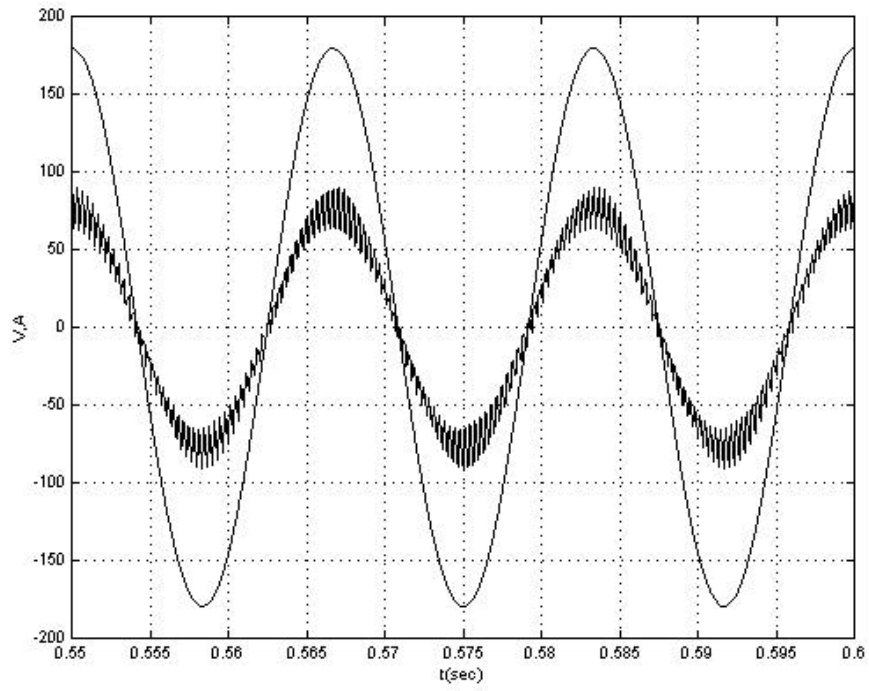
As to the duty ratios of  $S_1, S_2, S_3, S_4, S_5, S_6$ , they are the sum of two parts. The first part is obtained by comparing  $m_k(t)$  with a positive slope sawtooth wave. The second part is the same as that obtained from  $d_0$ .

Fig. 3.3 shows some results of the converter for  $V_o = 500 \text{ V}$ ,  $d_0 = 0.58$ , and  $P_o = 4 \text{ kW}$ . From Fig. 3.3(a) one can see the duty cycle controls. Fig. 3.3(b) and 3.3(c) show the waveforms of a-phase voltage and current as well as the output voltage.

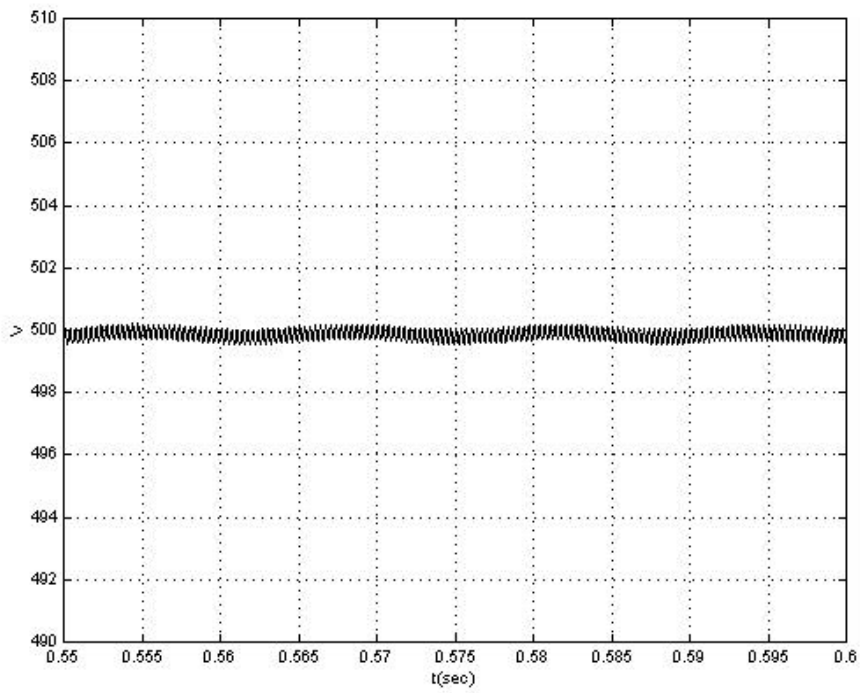
Similarly Fig. 3.4 shows the corresponding step down case where  $V_o = 48\text{ V}$ ,  $d_0 = 0.11$  and  $P_o = 4\text{ kW}$ . One can see that application of the derived open loop duty ratio control laws indeed work very well as expected.



(a)

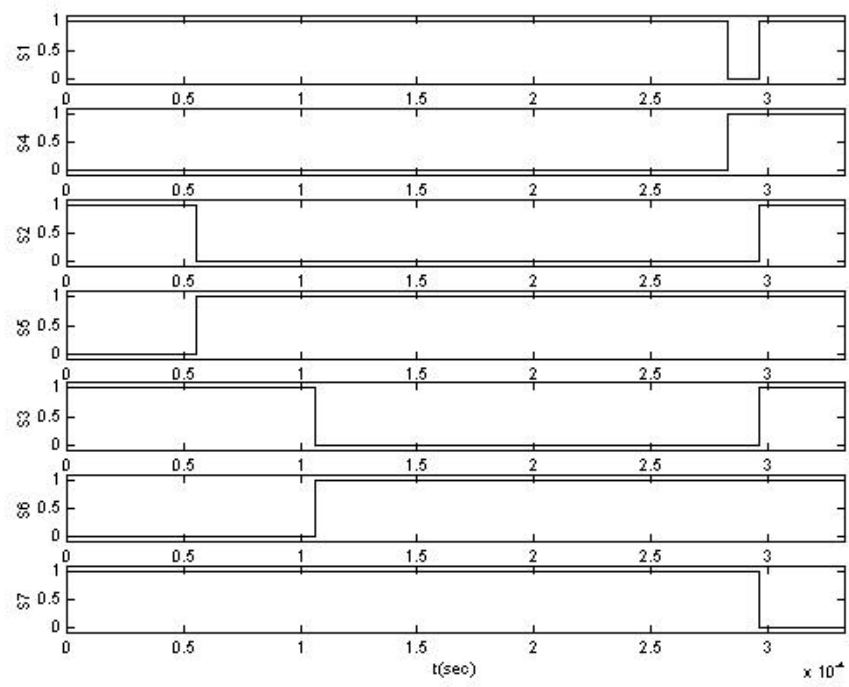


(b)

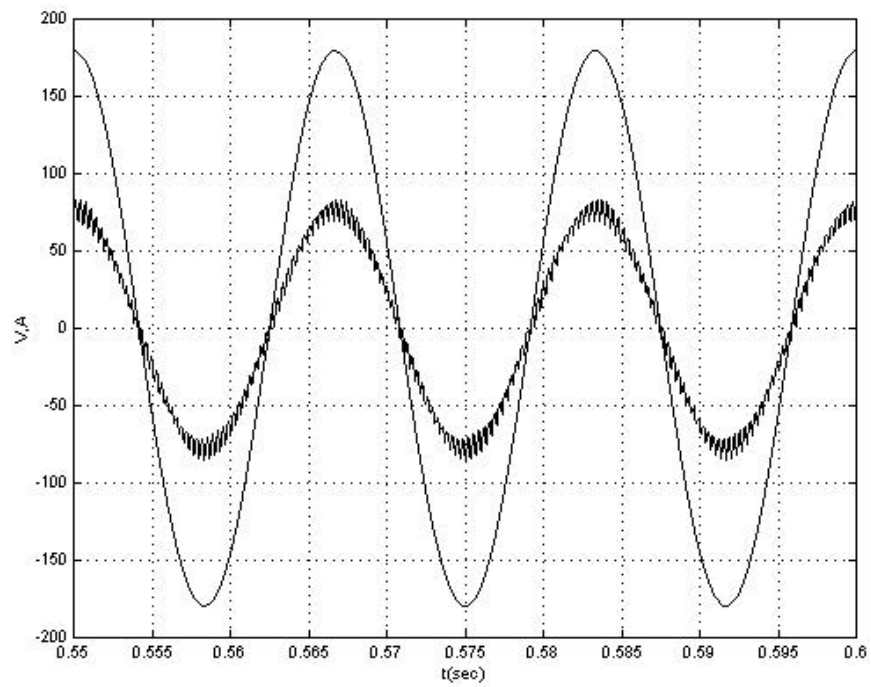


(c)

Fig. 3.3 Waveforms of (a) gating signals of all switches, (b) phase voltage  $e_a(t)$  and current  $5i_a$ , (c) output voltage  $v_o(t)$  under step up operation

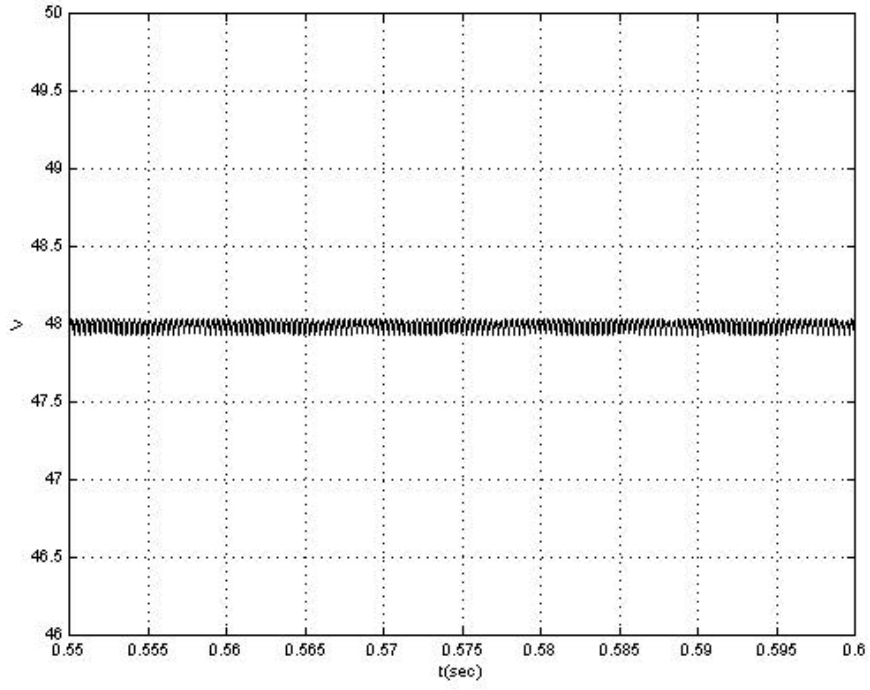


(a)



(b)





(c)

Fig. 3.4 Waveforms of (a) gating signals of all switches, (b) phase voltage  $e_a(t)$  and current  $5 i_a$ , (c) output voltage  $v_o(t)$  under step down operation

Finally, the duty cycle control to output voltage transfer functions for the step-up case are given as follows:

$$T_d(s) = \frac{2.715 \times 10^9 (s - 1431)(s + 60)}{\Delta_u(s)}$$

$$T_q(s) = \frac{8.369 \times 10^{11} (s - 1431)}{\Delta_u(s)}$$

$$T_0(s) = \frac{1.402 \times 10^8 (s - 2.133)(s^2 + 115.6 s + 1.556 \times 10^5)}{\Delta_u(s)}$$

$$T_{em}(s) = \frac{3.757 \times 10^9 (s + 157.41)}{\Delta_u(s)}$$

where

$$\Delta_u(s) = (s + 7.75)(s^2 + 111.1 s + 1.488 \times 10^5)(s^2 + 20.73 s + 2.236 \times 10^5)$$

Similarly, the corresponding transfer functions for the step-down case with  $V_o = 48 V$ ,  $D_0 = 0.11$  and  $P_o = 4 kW$  are listed below.

$$T_d(s) = \frac{4.126 \times 10^8 (s - 1431)(s + 60)}{\Delta_d(s)}$$

$$T_q(s) = \frac{1.587 \times 10^{11} (s - 1431)}{\Delta_d(s)}$$

$$T_0(s) = \frac{7.0953 \times 10^7 (s - 7.038)(s^2 + 101.4 s + 1.84 \times 10^5)}{\Delta_d(s)}$$

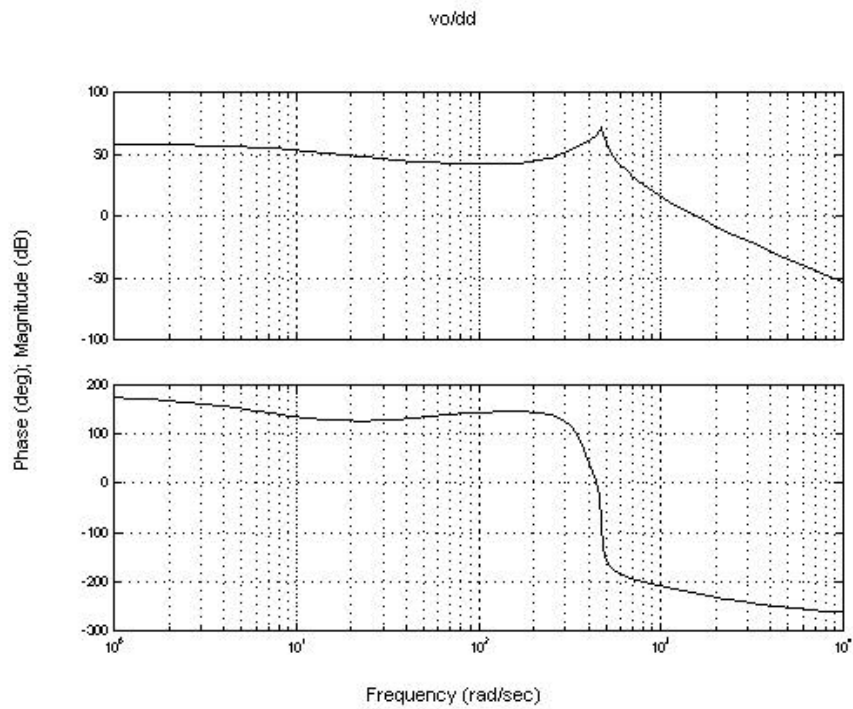
$$T_{em}(s) = \frac{1.408 \times 10^9 (s + 157.41)}{\Delta_d(s)}$$

where

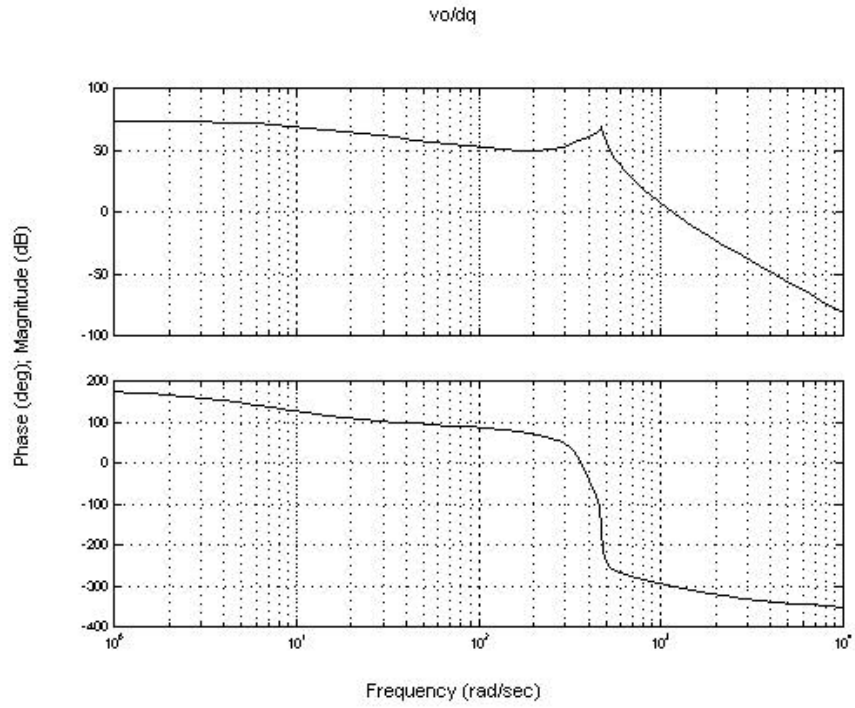
$$\Delta_d(s) = (s + 2037)(s^2 + 93.1 s + 2657)(s^2 + 106.6 s + 1.854 \times 10^5)$$

For convenient reference, Figs. 3.5 and 3.6 show the Bode plots for the two cases, respectively.

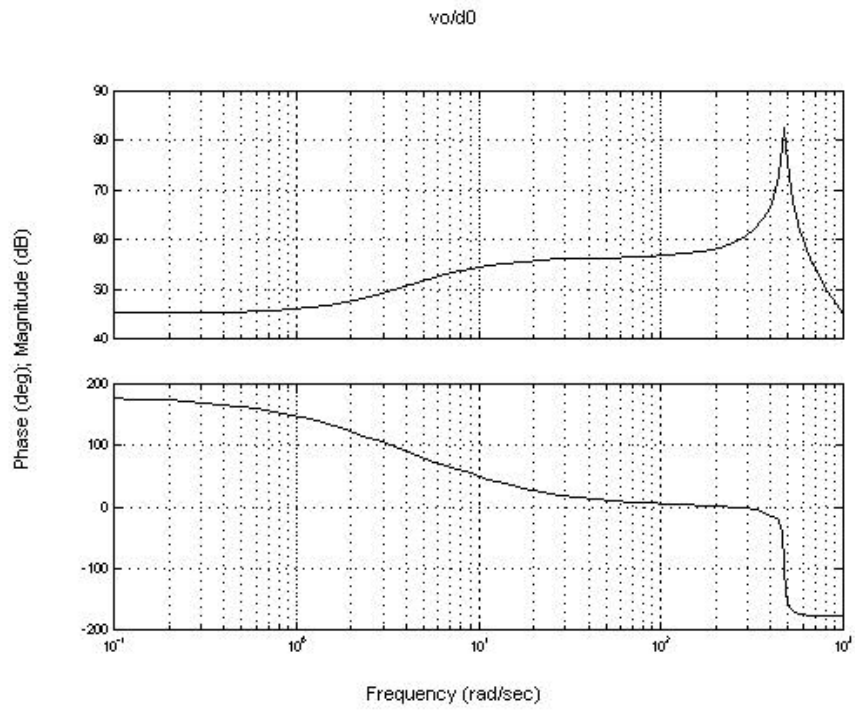
From the above results, it is very interesting to see that a right half plane zero also exists in the transfer functions of the proposed AC/DC converter. This implies that the converter dynamic has a time delay from the control to the output.



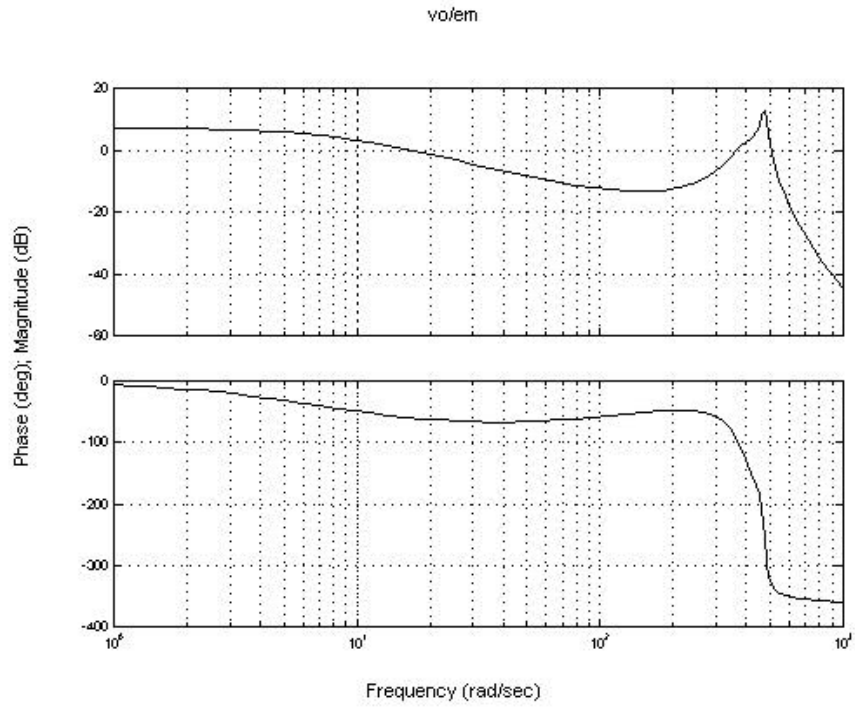
(a)



(b)

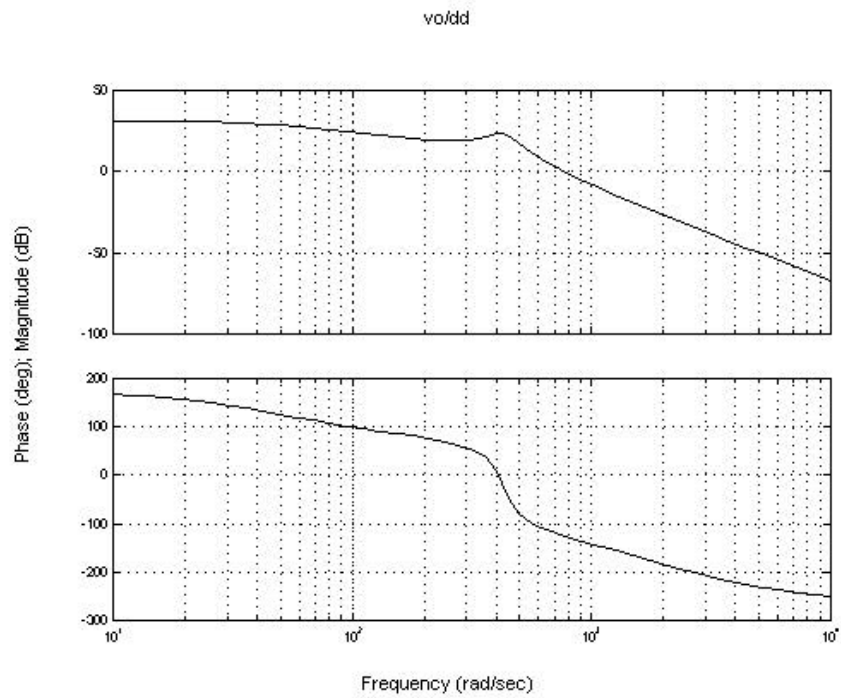


(c)

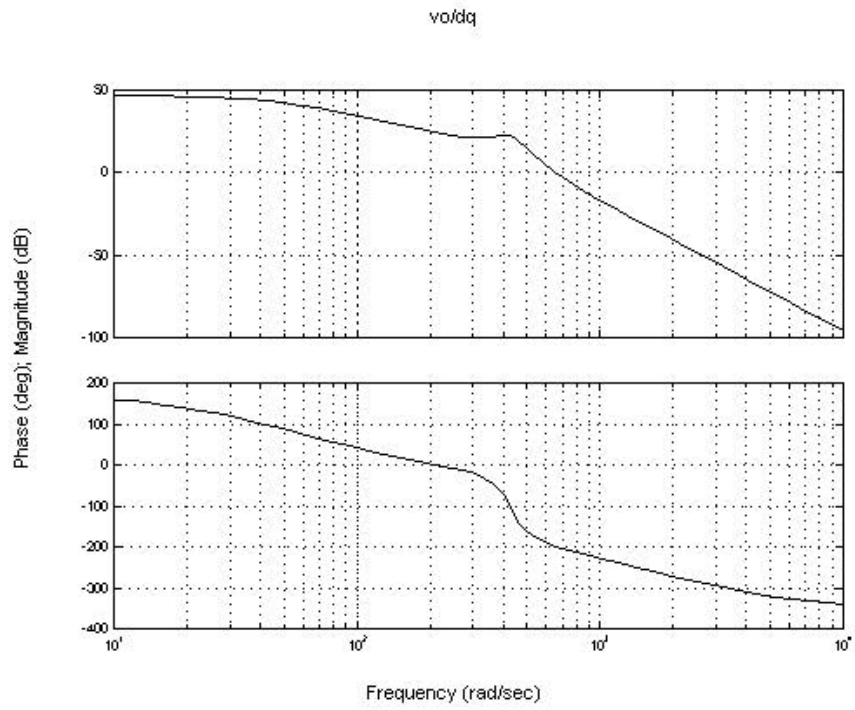


(d)

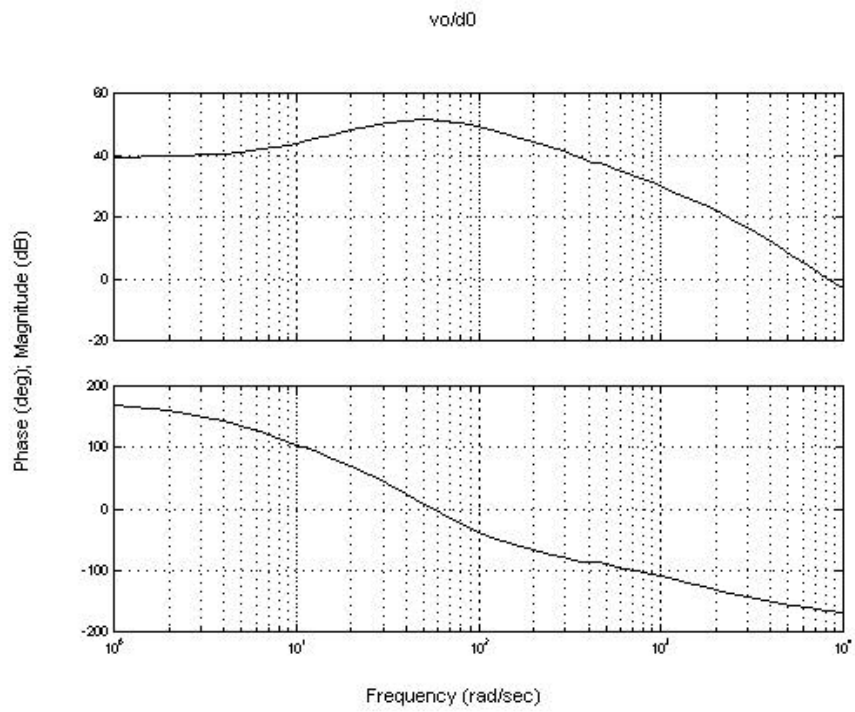
Fig. 3.5 Bode plots of (a)  $T_d(s)$ , (b)  $T_q(s)$ , (c)  $T_0(s)$ , (d)  $T_{em}(s)$  under step up operation



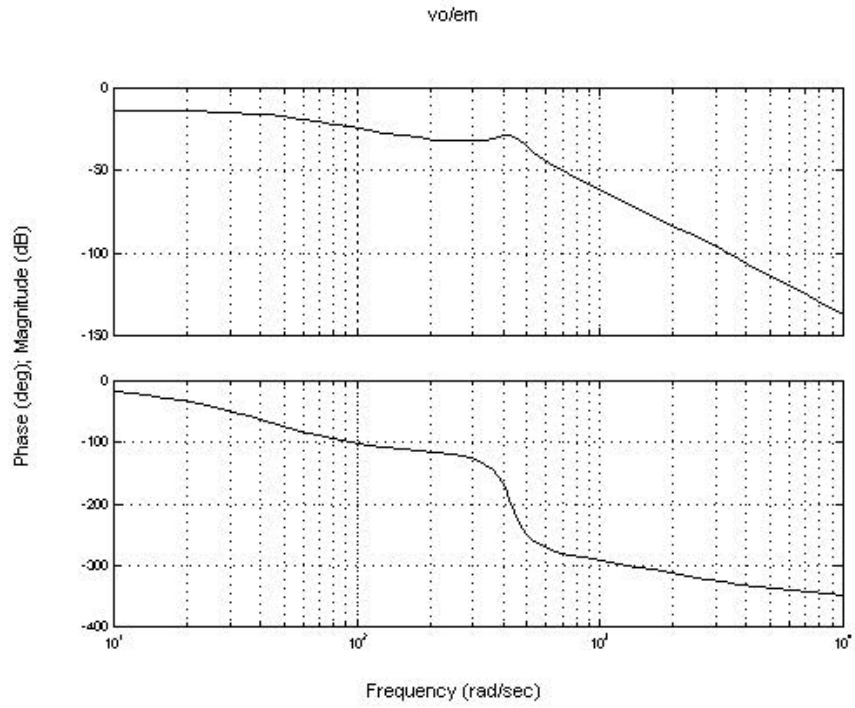
(a)



(b)



(c)



(d)

Fig. 3.6 Bode plots of (a)  $T_d(s)$ , (b)  $T_q(s)$ , (c)  $T_0(s)$ , (d)  $T_{em}(s)$  under step down operation